IEEE Access
Multidisciplinary ⋮ Rapid Review ⋮ Open Access Journal

Received 13 August 2023, accepted 20 September 2023, date of publication 24 October 2023, date of current version 27 October 2023.

Digital Object Identifier 10.1109/ACCESS.2023.3321272

TOPICAL REVIEW

Breast MRI Segmentation by Deep Learning: Key Gaps and Challenges

KHADIJEH ASKARIPOUR AND ARKADIUSZ ZAK
Department of Biomechatronics, Gdańsk University of Technology, 80-234 Gdańsk, Poland

Corresponding author: Arkadiusz Zak (arkadiusz.zak@pg.edu.pl)

The work of Khadijeh Askaripour was supported by the Nobelium Joining Gdańsk University of Technology (GUT) Research Community under Project 11/2020/IDUB/I.1.

ABSTRACT Breast segmentation in magnetic resonance imaging (MRI) slices plays a vital role in early diagnosis and treatment planning of breast anomalies. Convolutional neural networks with deep learning have indicated promise in automating this process, but significant gaps and challenges remain to address. This PubMed-based review provides a comprehensive literature overview of the latest deep learning models used for breast segmentation. The article categorizes the literature on deep learning based on input modalities, use of labeled/unlabeled data during training, and different architectures. Additionally, it describes more complex frameworks structured using hierarchical, ensemble, or fused learning. Then, MRI processing approaches, key aspects of convolutional neural networks, and key gaps and challenges are focused. The need for large breast MRI datasets with accurate annotations and the generalization of the proposed structures to diverse and comprehensive datasets are among the gaps.

INDEX TERMS Breast cancer, computer-aided diagnosis, CNNs, MRI processing, review.

I. INTRODUCTION

According to estimates by the American Cancer Society in 2022 [1], there would be 287,850 invasive cases of breast cancer and 43,250 deaths among women in the United States, as visualized in Fig. 1. Additionally, there would be 51,400 cases of ductal carcinoma in situ (DCIS), a stage-0 breast cancer confined to the ducts of the breast with the potential to progress to an invasive type. Long-term follow-up studies of untreated DCIS cases have reported rates of progression to invasive breast cancer ranging from 10% to 53%.

Early diagnosis of breast anomalies is crucial for high survival rates in breast cancer. Since breast cancer often exhibits no symptoms in its early stages, the American Cancer Society recommends annual screening at age 40 for women at average risk and at age 30 for women at high risk [1]. Among different nondestructive evaluation techniques [2], mammography is the primary imaging modality, while magnetic resonance imaging (MRI) serves as a supplementary method for high-risk or dense-breasted women [3].

The associate editor coordinating the review of this manuscript and approving it for publication was Rajeswari Sundararajan.

MRI techniques such as T1/T2-weighted imaging, diffusion-weighted imaging (DWI), and dynamic contrast-enhanced (DCE) imaging provide valuable information on different breast structures [4]. Combined as multi-parametric MRI, these techniques enhance the segmentation accuracy [5]. DCE-MRI, in particular, has shown promising results in early diagnosis for women with extremely dense breast tissues [6]. Contrast agents are used in DCE-MRI to improve visibility, and images are captured in 3D at different time points. Representative slices from axial T1-weighted (T1W) time-signal curves, pre-contrast, and first post-contrast sequences are displayed in Fig. 2.

Analyzing MRI data for tumor diagnosis is challenging for radiologists due to the large data volume. Additionally, various imaging artifacts can be introduced into breast MRIs, such as background noise, movement artifacts, chemical shift artifacts, incorrect patient positioning artifacts, magnetic susceptibility artifacts, and aliasing artifacts [8]. Therefore, the implementation of a computer-aided diagnosis (CAD) system becomes crucial to assist radiologists and physicians in analyzing breast MRI and expediting the diagnosis process. This analysis involves preprocessing, segmentation,

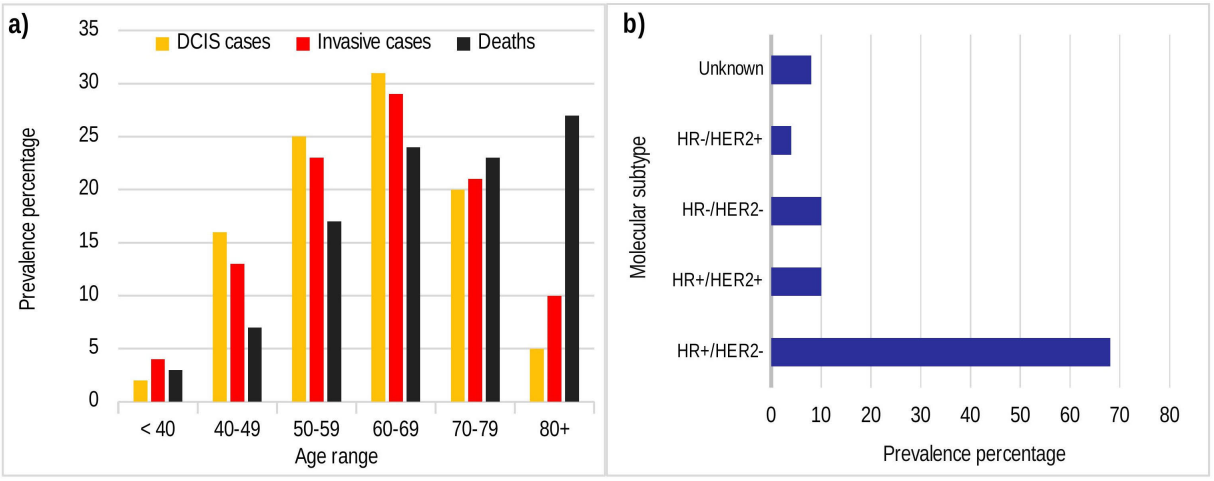

FIGURE 1. a) Age distribution of DCIS cases, invasive cases, and mortality in breast cancer patients in the United States in 2022; b) Distribution of breast cancer subtypes based on molecular traits in the United States from 2015 to 2019 [1].

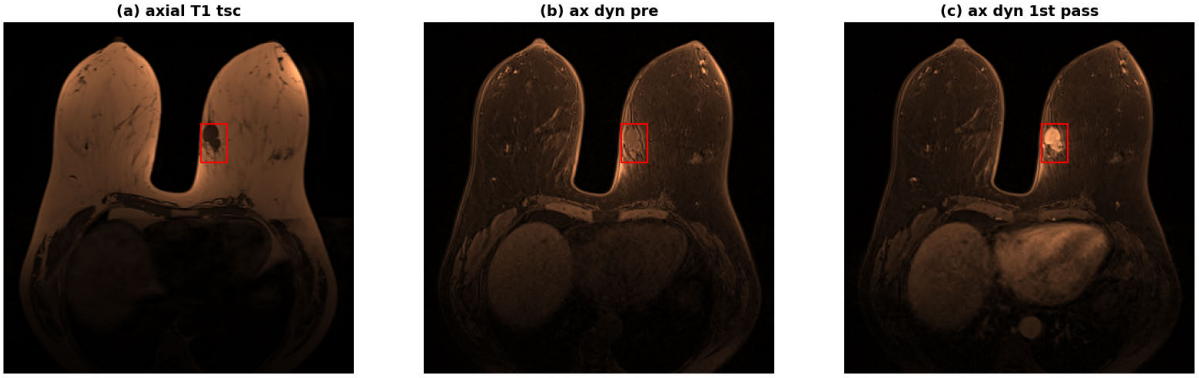

FIGURE 2. MRI modalities from the publicly available Duke database [7] showing images of patient 112, with a bounding box marking the suspicious area.

region of interest (ROI) detection, classification into benign or malignant categories, and identification of molecular subtypes, as shown in Fig. 3.

Automatic segmentation of breast structures, as shown in Fig. 3, within a CAD system plays a critical role in accurate cancer diagnosis. Several factors contribute to this: a) breast MRI slices encompass adjacent organs such as heart, liver, and pectoral muscles; b) tumors may exhibit lower contrast compared to normal blood vessel tissues; c) breast MRI exhibits variability due to the utilization of different MRI acquisition protocols; and d) automated segmentation can exclude unwanted areas and measure breast density and its temporal gradients as a cancer risk factor, while manual delineations being time-consuming and prone to error. To address these challenges, CAD systems frequently leverage machine learning (ML), a subset of artificial intelligence. The learning process can be either unsupervised, as in the case of fuzzy c-means [9], [10], or supervised, employing algorithms such as support vector machines [11], random forests [12], and logistic regression [13]. Manual feature extraction, being time-consuming and tedious to develop, was a necessary step in traditional machine learning [14]. However, deep learning algorithms based on convolutional neural networks have revolutionized this field by enabling direct learning and recognition of relevant features from the images [15].

This review aims to provide an overview of the latest advancements in deep learning-based techniques for automatic MRI segmentation in the field of breast cancer. It highlights the current state of the field while emphasizing the existing gaps and challenges. The increasing trend in the use of artificial intelligence regarding breast cancer based on the number of published reviews is depicted in Fig. 4 (a). Furthermore, Fig. 4 (b) shows the original research articles that are the basis of the current review. Additionally, Fig. 5 shows the literature content presented in the next section, followed by sections on *MRI processing approaches*, *key aspects of CNN*, and *key gaps and current challenges*. Finally, the review concludes with *conclusions and future directions*.

II. LITERATURE REVIEW

This section presents a summary of key findings, methodologies, and approaches related to breast MRI segmentation using deep learning models. Table 1 showcases notable studies in the literature, where CNN-based models are utilized to perform segmentation by classifying individual

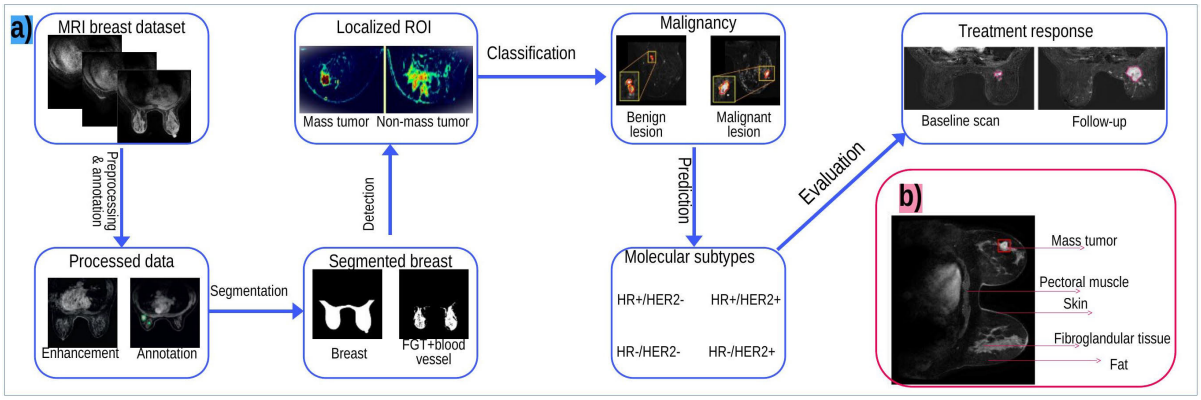

FIGURE 3. a) Image analysis procedure for breast MRI data; b) Breast structure.

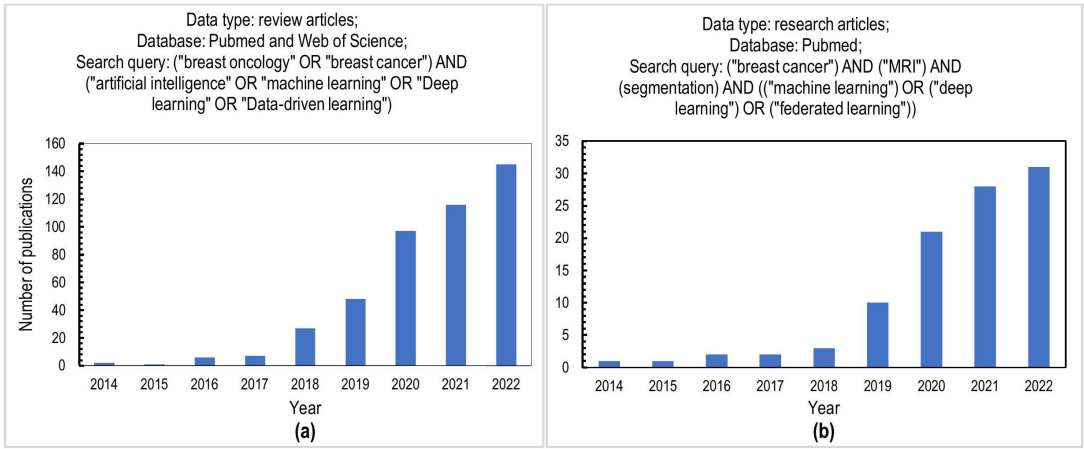

FIGURE 4. a) Review articles published on artificial intelligence applied to breast cancer; b) Research articles specifically focused on the subject of current review.

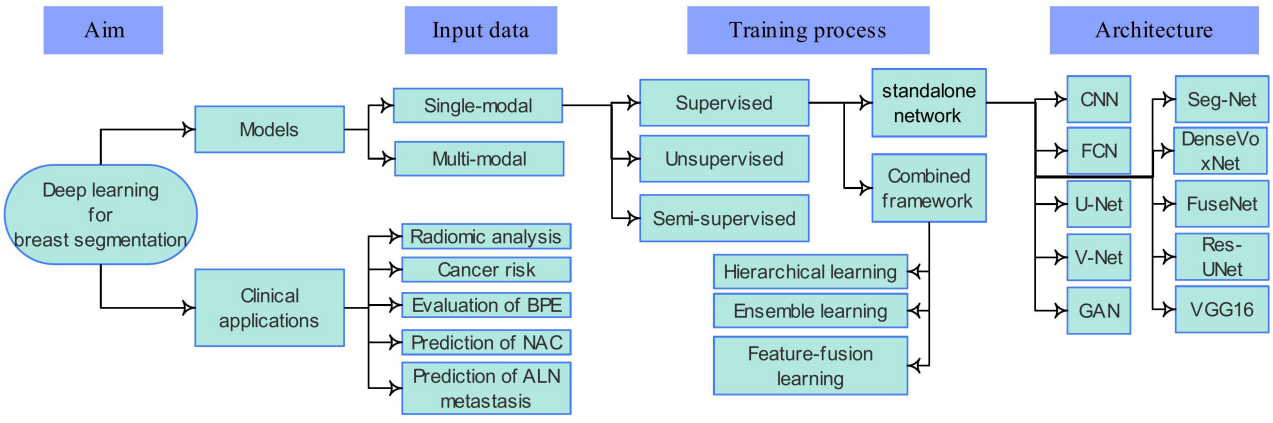

FIGURE 5. Overview of the state-of-the-art knowledge organization. (BPE→background parenchymal enhancement; NAC→neoadjuvant chemotherapy; ALN→axillary lymph node.)

pixels through a sliding window technique. The main steps for image segmentation includes: a) MRI data preprocessing; b) model development and training; c) model evaluation; d) inference; and e) post-processing. Multi-modal models integrate information from multiple input MRI modalities such as T1, T1 contrasted, and T2, while single-modal ones use only one type of input modality.

A. MULTI-/SINGLE-MODAL MODELS

Segmenting breast tumors in single-modal images is challenging due to the limited tumor morphology and the difficulty in distinguishing between tumors and normal blood vessels [23]. On the other hand, multi-modal images contain richer tumor information, as tumors exhibit distinct morphological or grayscale differences from other tissues.

TABLE 1. Deep learning (DL) models for breast segmentation.

Aim (source)	DL model and Input	Performance evaluation	Processing approaches	Key findings
FGT segmentation [16]	Models: 2C U-Nets (hierarchical learning), 3-C U-Net. Dataset: 132 T1 DCE-MRIs of 66 non-cancerous patients. Reference: manual annotations.	Dice similarity coefficient (DSC); Pearson's correlation between breast density values.	N4 bias-field correction using the breast mask; manual thresholding to select FGT voxels; image reorientation; image mirroring for left breast.	3C U-Net→DSC: 0.85, Pearson's correlation: 0.974; 2C U-Nets→DSC: 0.811, Pearson's correlation: 0.957.
Tumor segmentation [17]	Models: 2D Seg-Net and U-Net. Dataset: 86 T1 DCE-MRIs of 43 cancer patients. Reference: manual annotations.	Mean intersection over union (IoU); binary cross entropy; one-sided Mann-Whitney U test.	N4ITK bias-field correction; augmentation using random translations, rotations, flips, and scale; linear transformations.	Seg-Net → IoU: 68.88%, Loss: 0.053; U-Net →IoU: 76.14%, Loss: 0.002.
3D FGT segmentation [18]	Model: U-Net and patch DCNN based GAN. Dataset: bilateral breast pre-contrast MRIs of 100 patients. Reference: manual annotations.	DSC and Jaccard index (JI).	Normalization; rescaling; and resizing.	DSC: 87.0 ± 7.0% and JI: 77.6 ± 10.1%.
Mass segmentation [19]	Model: a 3D modified FuseNet based on U-Net. Dataset: T1 DCE-MR and T2W images from 313 patients. Reference: manual annotations for central slices.	Dice similarity, sensitivity, and relative area difference (RAD).	Resizing; normalization; combination of cross-entropy loss and Dice loss for the loss function.	Proposed model→Dice: 77.6 ± 0.3, sensitivity: 84.4 ± 0.7, and RAD: 30.9 ± 1.6. Respective values 74.9 ± 0.2, 82.2 ± 0.4, and 37.9 ± 2.5 for Fuse-UNet.
Tumor segmentation [20]	Model: a MHL framework via the U-Net structure. Dataset: T1W pre-contrast and first post-contrast MRIs of 272 patients. Reference: FCM segmentation using cuboid bounding box.	Mean DSC; Sensitivity (SEN); and Positive Predictive Value (PPV).	Image normalization; image reorientation; random resizing for data augmentation; cropping; or curve fitting and active contour based method. Manual annotations of the right and left nipples.	DSC: 71.76 ± 24.19, SEN: 75.04 ± 23.12, PPV: 77.33 ± 21.05. Better performance compared with random forest based method, patch-based CNN, U-Net, and V-Net.
3D lesion segmentation [21]	Model: multi-modal, ensemble learning via modified U-Nets. Dataset: 46 cases (3D T1W) from the TCGA-BRCA dataset. Reference: manual annotations for 2 lesions.	Mean DSC; Hausdorff Distance (HD); False Positive Rate (FPR); AdaDelta optimizer, and a threshold of 0.5.	Breast mask generation using skin-air boundary detection; zero padding; zero-mean unit-variance intensity normalization; balanced patch extraction.	DSC of 0.79 ± 0.172 for the proposed model.
Tumor segmentation [22]	Model: Res-Unet. Dataset: 1000 cancer patients under axial T1W DCE-MRI. Reference: manual and inference annotations.	DSC and intraclass correlation coefficient (ICC); Adam optimizer, DSC and cross-entropy based loss function.	Random zoom, scale intensity value, shift intensity range, Gaussian noise, crop fore/background, rotation, elastic transformation. Normalization and respacing.	DSC: 0.89; ICC>0.95 for tumor diameter and ICC>0.80 for tumor volume.
3D tumor segmentation [23]	Model: DenseVoxNet for coarse and a pseudo-Siamese network for fine segmentation. Dataset: T1W and T1-contrasted MRIs of 590 patients. Reference: manual.	Sensitivity, DSC, and absolute relative volume difference (ARVD). Dice Loss; Adam optimizer.	Image normalization.	DSC→T1C: 90.49 ± 1.89; T1: 85.07 ± 3.61.

2C U-Nets→Two Consecutive U-Nets; 3-C U-Net→3-Class U-Net; DSC→Dice Similarity Coefficient; FGT→Fibroglandular Tissue; IoU→Mean Intersection over Union; GAN→ Generative Adversarial Network; JI→Jaccard Index; DCNN→Deep Convolutional Neural Network; T1W and T2W→ T1 Weighted and T2 Weighted; MHL→Mask-guided Hierarchical Learning; FCM→Fuzzy C-Means; PSN→Pseudo-Siamese Network; T1C→T1 Contrasted.

Regarding multi-modality, Piantadosi et al. [24] incorporated the 3 time points (3TP) approach into the U-Net architecture for lesion segmentation in MRI slices. They inputted temporal acquisitions before and after the contrast agent injection (T = 0, 2, and 6 min), and achieved a median dice similarity coefficient of 61.24%. Khaled et al. [21] explored an ensemble U-Net framework for lesion segmentation using three U-Net models with different inputs: 3TP acquisitions, a full series of images, and pre, last, and standard deviation images of the full series. They also incorporated a breast mask in all models and replaced U-Net convolutional blocks with residual basic blocks. Hirsch et al. [25] achieved radiologist-level performance with a 3D U-Net, using a large training set of 60,108 benign breast and 2,455 malignant breast images. The input MRI included the first postcontrast image, T1 postcontrast minus precontrast image

(DCE-in), washout (DCE-out), and a reference created by radiologists.

Deep learning models can be classified into supervised, semi-supervised, or unsupervised based on their use of labeled and/or unlabeled data during training.

B. SUPERVISED MODELS

Over the past decade, supervised deep convolutional neural networks (CNNs) have consistently demonstrated superior performance compared to the prevailing state-of-the-art methods in numerous visual recognition tasks [26]. These techniques aim to automatically extract meaningful features from input images. Low-level features such as texture and edge detection are captured in the initial layers, while subsequent layers apply convolutional kernels to evolve the feature maps, resulting in high-level features near the output layer. Moeskops et al. [27] segmented the breast's pectoral muscle efficiently in 34 T1-MRIs using a fully CNN applied on a combination of brain MRI, breast MRI, and cadiac CTA. Guo et al. [28] utilized a CNN-SVM network for MRI breast tumor segmentation, where the label output of a trained CNN was fed into a support vector machine (SVM). Various learning architectures based on U-Net, Seg-Net, FuseNet, or GAN, have been applied for breast MRI segmentation.

1) U-NET-BASED MODELS

The majority of CNN models for automatic segmentation use the U-Net architecture [29]. U-Net extends the concept of a fully CNN [30] by incorporating up-sampling layers after standard CNN layers. Ronneberger et al. [29] employed elastic deformation for extensive data augmentation to address limited training data, and utilized a weighted loss function for handling touching objects. Later, Çiçek et al. [31] applied this U-Net architecture to construct a 3D network, training it on 3D volumes with sparse annotations. Preferentially, 3D models are chosen to capture both intra-slice and inter-slice tumor characteristics.

a: STANDALONE VERSUS COMBINED LEARNING

Deep learning can be achieved through standalone or combined frameworks. In standalone networks, input data is processed to extract high-level features, enabling output predictions without additional connections. On the other hand, a combined framework can be structured using hierarchical learning, ensemble learning, or feature fusion learning. Both standalone and combined frameworks are essential in deep learning, offering flexibility and adaptability for diverse applications. Yue et al. [22] developed an efficient standalone network called Res-UNet by incorporating residual blocks in the encoder section and combining them with U-Net skip connections. Dalmış et al. [16] employed two U-Net based approaches, namely the two consecutive U-Nets (2C U-Nets) via hierarchical learning and the 3-class U-Net (3-C U-Net) as a standalone framework. The 2C U-Net segments the breast first, then follows with FGT segmentation. On the other hand, the 3-C U-Net simultaneously segments the entire volume into three classes: nonbreast tissue, breast FGT, and breast fat. The 3-C U-Net method demonstrated superior performance over traditional machine learning including an atlas-based algorithm.

b: HIERARCHICAL LEARNING

This approach entails training lower-level models to perform simple tasks and utilizing their outputs as input for higher-level models. In a segmentation approach by [20], first, a U-Net model using a pre-contrast image generated a breast mask, which serves as input to the next two-stage U-Net model. Then, a double U-Net framework utilized first post-contrast image and the subtraction image to achieve coarse-to-fine segmentation, resulting in a tumor mask. To address class imbalance, the authors introduced a dice-sensitivity-like loss function and a reinforcement sampling strategy. Peng et al. [23] devised a multi-modal hierarchical network that consists of two stages for segmentation of small tumors. The first stage introduced a novel 3D tiny object segmentation network (TOSN) based on DenseVoxNet [32] to capture tumor boundary details. Second stage used a bidirectional request-supply information interaction module (BD-RSIIM) to enable information exchange between sub-networks of two modalities. Qin et al. [33] employed a two-stage U-Net-based framework, in which the first stage applied a refined U-Net model to automatically delineate a breast ROI. The second stage enhanced the U-Net model by modifying the activation function, substituting batch normalization with group normalization, introducing a dense residual module using dilated convolution in the encoder, and replacing the original convolution blocks in the decoder with a recurrent attention block.

c: ENSEMBLE LEARNING

This approach combines the predictions of multiple individual models to improve the overall performance through techniques like averaging, voting, or stacking. Piantadosi et al. [34] made modifications to the original U-Net model by adjusting the output feature map to a single channel, employing size-preserving zero-padding, and incorporating batch normalization layers after each convolution. The modified model analyzed 2D MRIs in sagittal, coronal, and transversal planes using an ensemble approach with a voting technique. Khaled et al. [21] reported that the union operation of three U-Net models in an ensemble learning process achieved the most effective segmentation of primary lesions.

d: FEATURE FUSION LEARNING

This involves integrating features from multiple sources or models to enhance performance or provide a comprehensive representation of the input data. The U-Net++ framework was utilized to segment the breast region in DCE-MRIs of 75 patients, surpassing the performance of U-Net [35]. U-Net++ [36] improves upon the original U-Net architecture

by enhancing the skip connection with feature combination modules, enabling the fusion of features from different levels through superposition. It also incorporates a deep supervision scheme that connects the middle module to the final output, ensuring effective gradient propagation.

2) SEG-NET MODELS

The following single-modal, standalone architectures compare Seg-Net and U-Net performances for breast MRI segmentation. In certain instances, El Adoui et al. [17] demonstrated that the U-Net model achieved higher accuracy in predicting the segmentation of 2D slices compared to human-generated segmentation. Conversely, the qualitative results obtained by Seg-Net were not closely aligned with the ground truth. This disparity was attributed to the fact that Seg-Net is better suited for multiclassification tasks, such as applications related to autonomous car. Moreover, Carvalho et al. [37] utilized U-Net and Seg-Net architectures for tumor segmentation in 2D T1 and T2 images. Seg-Net demonstrated superior performance with a dice coefficient of 97.55% and an IoU score of 95.30% when training with T1 images and testing with T2 images. Therefore, segmentation performance using Seg-Net or U-Net was varied based on the input.

3) GAN-BASED MODELS

Generative adversarial networks (GANs) are deep neural network architectures that consist of two competing networks [38]. Ma et al. [18] introduced a GAN-based approach for precise fibroglandular tissue (FGT) segmentation, essential for quantitative analysis of background parenchymal enhancement (BPE) in MRI and assessing breast cancer risk. It utilizes an enhanced U-Net as a generator to produce FGT candidate regions, while a patch deep convolutional neural network (DCNN) functioning as a discriminator to assess the credibility of the generated FGT region. The FGT areas segmented by the proposed GAN model provided improved quantification of BPE compared to those by the baseline U-Net.

4) FuseNet MODELS

Li et al. [19] applied two modifications on FuseNet [39] for breast mass segmentation. First, a FuseNet-like network is built upon U-Net, named FuseOrigin-Unet. Second, a channel-wise concatenation is implemented to fuse different imaging modalities, and convolution kernels for each layer are halved in encoder, named FuseUNet. Therefore, their model was applied to multi-modal MRIs, with the T1C processed as the primary modality for segmentation and T2W as assistant. An attention block was employed to extract supervision information from the primary modality and then to choose relevant information from assistants.

C. UNSUPERVISED MODELS

The goal of unsupervised learning is to discover the ROI in images without any manual annotations or bounding boxes during training. Parekh et al. [4] employed a stacked sparse autoencoder (SSAE) multiparametric deep learning network that utilizes breast tissue signatures from various MRI modalities (T1-weighted, T2-weighted, DCE imaging, and DWI) as inputs for unsupervised breast segmentation.

D. CLINICAL APPLICATIONS OF SEGMENTATION

Segmentation in medical imaging accurately delineates and identifies specific structures or regions of interest, enabling various clinical applications such as radiomic analysis, treatment response, disease progression, and cancer risk assessment.

1) RADIOMIC ANALYSIS

Radiomics involves extracting and analyzing quantitative features from breast MRIs. In their study, Spuhler et al. [40] employed a U-Net model to segment lesions in breast DCE-MRIs, which was then utilized as input for the radiomics model.

2) TREATMENT RESPONSE

Breast tumors automatically segmented using a U-Net model in the third post-contrast images were utilized to predict the likelihood of systemic recurrence within three years after neoadjuvant chemotherapy (NAC) operation in patients with triple-negative breast cancer [41].

3) DISEASE PROGRESSION

Axillary lymph node metastasis refers to the spread of cancer cells from the primary tumor site to the lymph nodes located in the axilla (armpit) region. Gan et al. [42] employed automatic segmentation to delineate axillary regions on post-neoadjuvant chemotherapy DCE-MRIs.

4) CANCER RISK

Accurate breast density assessment, as an indicator of breast cancer risk, was achieved through a supervised 3D U-Net segmentation strategy using fat- and water-only images [43]. Similarly, increased background parenchymal enhancement (BPE) linked to higher breast cancer risk was classified by employing radiomics features extracted from segmented images using a modified V-Net model [44]. The BPE region was identified using thresholding values in the subtraction of the pre- and post-contrast T1W images and the segmented FGT mask. The main steps required for segmentation, as shown in Fig. 6, are addressed in more details in the subsequent sections.

III. MRI PROCESSING APPROACHES

T1-/T2-weighted imaging, DWI, and DCE-MRI are key MRI modalities employed in breast cancer diagnosis. Despite each modality consisting of numerous slices, they often lack sufficient information to differentiate between tumors and breast nodules, which exhibit similar sizes and shapes. The utilization of multi-modal images becomes crucial in accessing a broader dataset for identifying abnormalities.

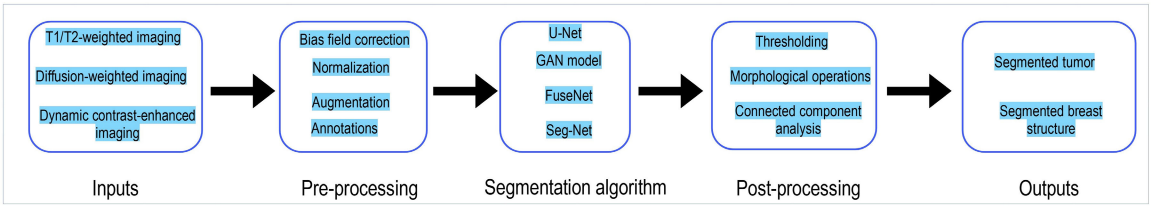

FIGURE 6. Sample segmentation process of breast MRIs.

Consequently, the application of image processing techniques becomes necessary.

A. INPUT MRI DATA

The DL algorithm uses multi-modal MRIs and mask labels as input data, and models with multi-modal inputs are more effective than those with single-modal inputs [19]. Including the precontrast image as input provided anatomical information, excluding enhancements from the heart in the chest region [45]. Similarly, incorporating the contralateral subtraction image as input helped eliminate false positives from parenchymal enhancements, important for radiologists' interpretation and deep learning models. Ground truth labels are generated manually by experts using graphical software to assess segmentation accuracy. When evaluating effect of the tumor alone and different annotation boxes [10], the smallest box containing proximal peritumor tissue showed the highest accuracy. Researchers have applied various techniques on raw data to enhance result reliability.

B. PROCESSING TECHNIQUES

1) PREPROCESSING

This step plays a pivotal role in image segmentation and is mandatory to remove marks, labels, non-breast tissues, and black areas. Some commonly-used techniques (refer to Table 1) are as follows: normalization; rescaling and resizing; augmentation using geometric transformations, such as rotations, flips, or translations; and motion correction using 3D rigid and non-rigid image registration [11], [46]. The role of preprocessing in highlighting the tumor region and removing the non-breast areas is shown in Fig. 7.

2) DURING-PROCESSING

Data balancing is crucial in medical imaging due to the significant imbalance between voxels representing lesioned and healthy tissues. Galli et al. [46] tackled this challenge by implementing an eras/epochs training schema that ensures an equal number of healthy and lesion slices are sampled during each training step. To balance the data, Yue et al. [22] employed a random selection method for cropping patches. The center point of the patches was chosen with equal probability either within the foreground or background area. Additionally, they applied various degrees of rotation (augmentation) during inference to the input data before feeding them into the model for evaluation. Patch extraction, transfer learning, and attention mechanisms are also among this type of techniques.

3) POST-PROCESSING

Morphological operations (e.g., erosion and dilation), thresholding, and connected component analysis can be utilized to refine segmentation result. Techniques like skin fold removal to improve fibroglandular tissue segmentation [47], retaining only the largest continuous regions of segmentation [48], eliminating outliers within connected regions [22], and applying a threshold of 0.35 with hole filling [43] have been implemented to enhance segmentation results.

IV. KEY ASPECTS OF CNN

This section explores the essential components and various basic architectures of CNNs, and offers insights into the core elements contributing to their success in breast MRI segmentation.

A. CNN COMPONENTS

Different CNN architectures can be designed by adjusting the parameters related to the components as following, depending on the specific segmentation task requirements and dataset characteristics.

1) CONVOLUTIONAL LAYERS

They perform convolution operation, which involves sliding a small matrix called a filter, to extract features from the input data.

2) ACTIVATION FUNCTIONS

They introduce non-linearity following each convolutional layer, and enable the network to learn complex patterns and make accurate predictions. Rectified Linear Unit (ReLU) has widely been used in hidden layers [29], [49]. Leaky ReLU activation function addresses a limitation known as the "dying ReLU" problem in standard ReLU and helps the network maintain the flow of gradients by introducing a small hyperparameter for negative input values [50]. Additionally, SoftMax or Sigmoid have been used at the final classifier layes [31], [35].

3) BATCH NORMALIZATION

This can enable end-to-end training with the same optimizing solver [49]. This technique was applied before each ReLU to enhance gradient flow leading to faster convergence [31] and

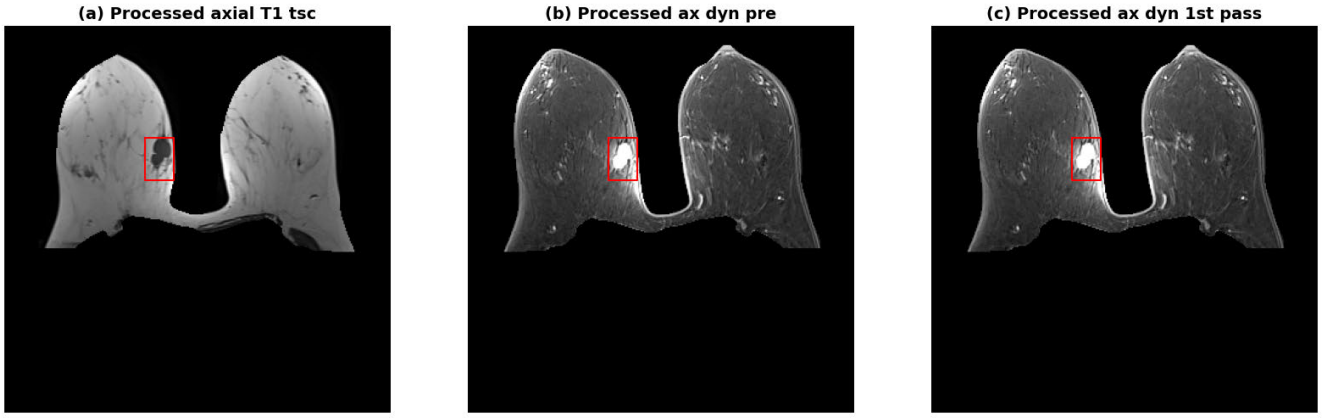

FIGURE 7. Preprocessing techniques applied to image modalities shown in Figure 2.

to reduce the internal covariate shift [39]. Additionally, it was applied after each ReLU block to improve training speed [51], to make the model robust to input variations [46], to reduce internal covariate shift [39], and to mitigate sensitivity to weight initialization [43].

4) POOLING LAYERS

They reduce the spatial dimensions of the feature maps through operations like max-pooling or average pooling, leading to a reduction in the number of parameters in subsequent layers. This leads to improvement in training speed and overfitting prevention.

5) OPTIMIZERS

They determine parameter adjustments during training through gradient computation and application, with commonly used options including stochastic gradient descent [17], adaptive moment (Adam) [23], and Adadelta as an extension of AdaGrad [21].

6) SKIP CONNECTIONS

They create extra paths for backpropagation between network layers by concatenating feature maps from the encoder with feature maps in the decoder. These connections bypass network layers, preserving and reusing low-level information during upsampling.

7) DROPOUT

It is a regularization technique that randomly ''drops out'' a portion of the neurons during training to prevent overfitting and improve generalization. For instance, Hazirbas et al. [39] utilized dropout in both the encoder and decoder to enhance the network performance.

B. ARCHITECTURES

1) SEG-NET

SegNet, as shown in Fig. 8 (a), is an encoder-decoder architecture, wherein encoder layers correspond with the convolutional layers found in the VGG16 architecture [52]. The encoder uses max-pooling layers that store pooling indices to be used in the corresponding decoder layers for usampling. The decoder output is input to a multi-class softmax classifier, generating independent class probabilities for each pixel [49]. Seg-Net uses stochastic gradient descent (SGD) with backpropagation for optimization, and it typically employs a variant of cross-entropy loss to measure dissimilarity between the predicted segmentation map and ground truth labels [37].

In terms of advantages, the use of max-pooling indices during downsampling in SegNet enables accurate breast boundary delineation and tumor localization [17]. SegNet's ability to handle input images of various sizes is particularly beneficial for medical images with different resolutions and aspect ratios. However, when it comes to breast tumor segmentation in 2D slices, SegNet did not yield efficient results compared to U-Net [17]. This was attributed to its exclusive reliance on saved pooling indices during convolution. SegNet primarily focuses on local spatial details and may not fully capture the broader contextual information [53].

2) FuseNet

FuseNet follows an encoder-decoder architecture, where the encoder is a two-branch network that simultaneously extract features from complementary depth input and fuse them into main feature maps [39], with encoder parameters fine-tuned from the VGG 16-layer model. Fig. 7 (b) shows the related architecture. Li et al. [19] used T1C MRI as main modality as it highlights breast masses as well as irrelevant regions, and T2W as auxiliary modality as it helps to distinguish true breast masses from all the enhanced areas. In terms of advantages, FuseNet leverages information from multiple MRI sequences, thus enhancing the segmentation accuracy by capturing complementary features from different imaging modalities.

3) U-NET

The U-Net architecture, as shown in Fig. 8 (a), comprises a contracting pathway (encoder) to capture contextual information and an expanding pathway (decoder) that symmetrically aids precise localization [29]. U-Net incorporates skip

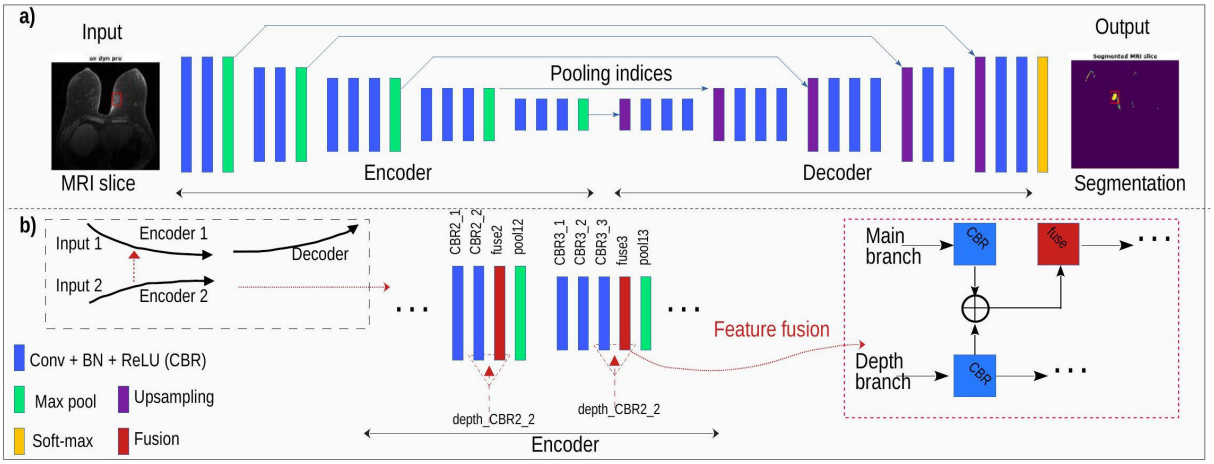

FIGURE 8. a) Seg-Net [49], b) FuseNet with dual input branches [39]. Fusion of depth branch and main branch feature maps is depicted by the red arrow. CBR2 and CBR3 refer to the second and third CBR layers.

connections between encoder and decoder to allow the model to capture both local and global contextual information.

In terms of advantages, U-Net is able to utilize complete images of any size, eliminating the need for patch division [16]. The architecture has demonstrated its ability to maintain resilience and robustness, even with a relatively limited amount of training data [35]. U-Net's design enables the combination of high-level information from the encoder with detailed spatial information from the decoder. On the other hand, U-Net exhibited limitations in accurately segmenting FGT due to challenges like fuzzy edges between FGT and neighbouring organs, false-positive segmentation of fat and pectoral muscle area in cases of low breast density, and under-segmentation in cases of high breast density [18]. When training data is limited, careful regularization techniques, such as dropout or data augmentation, should be employed to mitigate the risk of overfitting [54].

4) GAN

GANs have a generator and discriminator trained adversarially until convergence, as shown in Fig. 8 (b). The generator produces realistic segmentations, and the discriminator distinguishes real from synthetic ones. GANs generate realistic synthetic images, which can help in augmenting limited training data. This is particularly beneficial in cases where annotated data is scarce. Therefore, GANs can enable unsupervised learning, meaning they can learn from unannotated images. On the other hand, GANs for breast MRI segmentation may be sensitive to variations in breast shapes, sizes, and imaging protocols [18].

V. KEY GAPS AND CURRENT CHALLENGES

A. WELL-ANNOTATED BIG DATA

Well-annotated big data is crucial for training accurate segmentation models; however, the manual annotation process is time-intensive and requires expert knowledge. Key gap is the lack of large public datasets with comprehensive and accurate ground truths for training new deep learning models in breast MRI segmentation. Efforts initiated to bridge this gap include providing datasets on the "Cancer Imaging Archive" webpage, but further work is needed. Alternatively, there is growing interest in developing segmentation techniques independent of annotated data. Maicas et al. [55] combined globally optimal inference in a continuous space with deep learning. Other efforts in this direction can be found in the works of Meng et al. [56] and Parekh et al. [4].

Challenges in developing large public datasets with comprehensive and accurate annotations include inter-observer annotation variability and 3D annotation difficulty. Variability among radiologists in segmenting regions of interest in breast MRIs can introduce uncertainty in the ground truth annotations used for model training. For this reason, for instance, 266 malignant breasts were segmented by four radiologists, used for threshold tuning and testing by Hirsch et al. [25]. Regarding 3D annotations, neighboring slices often have inter-dependencies. Ensuring consistency and smooth transitions between slices during annotations is challenging for accurate segmentation. That is why, for example, Li et al. [19] labeled only the central slices having the largest cross-sections for masses.

B. INTER/INTRA VARIATIONS

Breast MRIs may significantly vary in shape, size, position, image appearance due to diverse imaging protocols, and patient characteristics, such as breast morphology, race, ethnicity, and disease features [56]. Consequently, there is a demand for robust deep learning models trained on large diverse datasets to handle such variabilities. To cite a few efforts, Hirsch et al. [25] utilized a large dataset featuring challenging cases involving small cancers and patients with breast implants. Dalmış et al. [16] employed a very small dataset but comprising different MRI acquisition protocols and breast types. Due to such variability, applying pre-trained deep learning models to diverse datasets is challenging and may require further generalization techniques.

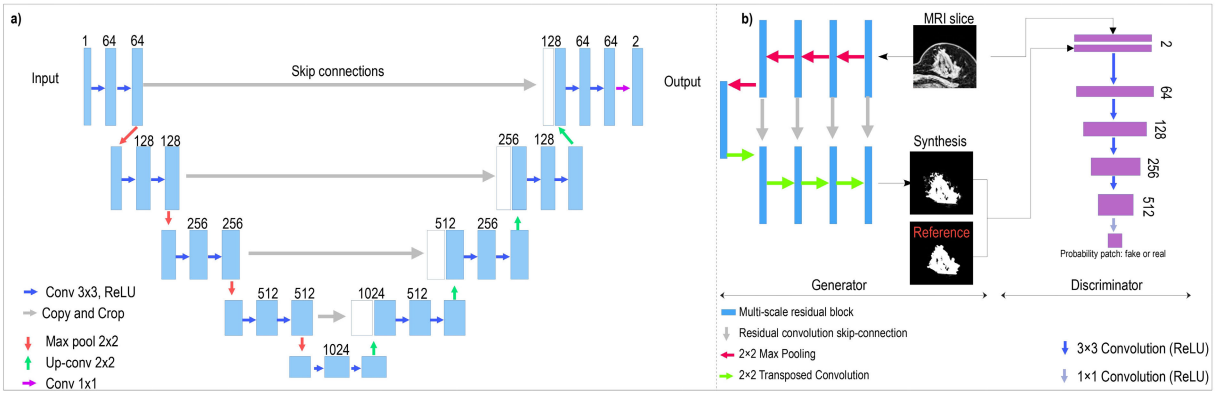

FIGURE 9. a) U-Net [29]. The blue boxes represent multi-channel feature maps, with the number of channels indicated on top of each box; b) GAN architecture [18].

C. GENERALIZATION TECHNIQUES

Generalizing deep learning models trained on a specific dataset to new, large, and diverse datasets is challenging [46]. Many researchers have tried to automate breast MRI segmentation by developing various DL techniques mostly trained on private small databases. Nonetheless, their application can be limited to their inputs, and model generalization remains a gap. Some researchers excludes patients with breast implants [43], or some use only 2D slices as inputs to learning algorithm [17]. Improving the generalization capabilities of algorithms through transfer learning [57], domain adaptation [58], or cross-dataset validation [59] is essential for clinical applications.

Various MRI modalities have been incorporated into the training algorithms, as single-modal images are unable to capture the complete tumor morphology without complementary information in other modalities. Single-modal segmentation of breast tumors leads to inaccurate tumor boundaries and false positive/negative candidates. In addition, 3D models are preferred over 2D models to capture the intra- and inter-slice features of the tumor [23]. The availability of large annotated datasets is crucial to improve the performance and generalization of models.

D. COMPLEX ANATOMY

The breast has complex anatomical structures such as tissue types, blood vessels, ducts and lesions. Accurate segmentation of these structures remains a challenge, especially in the presence of overlapping or unclear boundaries [43]. For instance, U-Net segmented th breast fat and the pectoral muscle as FGT in low-density breasts, while it was unable to segment the entire FGT region in high-density breasts [18]. Furthermore, breast MRI segmentation suffers from class imbalance, where the number of pixels belonging to the lesion or anomaly is significantly less than those pixels belonging to the non-target class. This can affect the model's ability to learn and generalize effectively. Therefore, advanced architectures for managing anatomical structures remains a gap that requires the integration of multiscale and contextual information.

VI. CONCLUSION AND FUTURE DIRECTIONS

The current review highlights latest trends in deep learning for automating breast MRI segmentation. Models based on U-Net, Seg-Net, FuseNet and generative adversarial network (GAN) architectures have been of interest to researchers for this purpose. The segmentation task forms the basis for further analysis of breast MRI including classification and diagnosis. Further future research is noteworthy to fill the gaps in some areas.

Many efforts have been aimed at automating breast MRI segmentation using various deep learning techniques mostly on private limited datasets. In order to indicate their efficiency for clinical applications, the performance of such models should also be investigated on diverse datasets. Despite some initiated efforts, large, diverse and well-annotated public breast MRI datasets are lacking in the literature. The algorithms trained and evaluated on multimodal compared to single-modal input have proven to be more accurate in differentiating between various normal tissues and lesions. Considering this fact, training on a large-scale dataset requires powerful computing equipment and long computing time. Efforts to reduce the computational complexity are much needed.

Various 2D and 3D CNNs have been developed using different architectures, with U-Net being the most common. By integrating different types of learning frameworks such as hierarchical, ensemble, or fused learning, more efficient frameworks for automating breast MRI segmentation have been introduced. Improving the performance of the proposed deep learning models and generalizing them to high-quality annotated datasets in breast MRI is very important for medical clinics. Open source codes can contribute to new algorithmic developments based on previous research by reproducing prior findings. Transfer learning allows models trained on a well-annotated dataset to generalize well to new sparsely annotated datasets of different feature space. Domain adaptation is another related technique capable of handling variability in imaging protocols and populations. Cross-validation can also help train unseen data and prevent overfitting. There is a lack of using such techniques in

breast MRI segmentation. Addressing the challenges requires collaborative efforts among researchers and medical experts to develop robust and reliable deep learning models.

Clinical implications of research findings are important. Since deep learning is considered complex and requires knowledge in computational engineering, it is imperative to develop simplified methods to enable interaction between models and clinicians.

REFERENCES

[1] *Breast Cancer Facts & Figures 2022–2024*, American Cancer Society, ATL, ACS, Washington, DC, USA, 2022.

[2] K. Askaripour and A. Zak, "A survey of scrutinizing delaminated composites via various categories of sensing apparatus," *J. Compos. Sci.*, vol. 3, no. 4, p. 95, Oct. 2019, doi: 10.3390/jcs3040095.

[3] D. Saslow, C. Boetes, W. Burke, S. Harms, M. O. Leach, C. D. Lehman, E. Morris, E. Pisano, M. Schnall, S. Sener, R. A. Smith, E. Warner, M. Yaffe, K. S. Andrews, and C. A. Russell, "American cancer society guidelines for breast screening with MRI as an adjunct to mammography," *CA, A Cancer J. Clinicians*, vol. 57, no. 2, pp. 75–89, Mar. 2007.

[4] V. S. Parekh, K. J. Macura, S. C. Harvey, I. R. Kamel, R. EI-Khouli, D. A. Bluemke, and M. A. Jacobs, "Multiparametric deep learning tissue signatures for a radiological biomarker of breast cancer: Preliminary results," *Med. Phys.*, vol. 47, no. 1, pp. 75–88, Jan. 2020.

[5] A. Meyer-Base, L. Morra, A. Tahmassebi, M. Lobbes, U. Meyer-Base, and K. Pinker, "AI-enhanced diagnosis of challenging lesions in breast MRI: A methodology and application primer," *J. Magn. Reson. Imag.*, vol. 54, no. 3, pp. 686–702, Sep. 2021.

[6] M. F. Bakker, S. V. de Lange, R. M. Pijnappel, R. M. Mann, and P. H. Peeters, "Supplemental MRI screening for women with extremely dense breast tissue," *New England J. Med.*, vol. 381, no. 22, pp. 2091–2102, 2019.

[7] A. Saha, M. R. Harowicz, L. J. Grimm, C. E. Kim, S. V. Ghate, R. Walsh, and M. A. Mazurowski, "A machine learning approach to radiogenomics of breast cancer: A study of 922 subjects and 529 DCE-MRI features," *Brit. J. Cancer*, vol. 119, no. 4, pp. 508–516, Aug. 2018.

[8] V. Fiaschetti, C. A. Pistolese, V. Funel, M. Rascioni, G. Claroni, F. Della Gatta, E. Cossu, T. Perretta, and G. Simonetti, "Breast MRI artefacts: Evaluation and solutions in 630 consecutive patients," *Clin. Radiol.*, vol. 68, no. 11, pp. 601–608, 2013.

[9] W. Chen, M. L. Giger, and U. Bick, "A fuzzy C-means (FCM)-based approach for computerized segmentation of breast lesions in dynamic contrast-enhanced MR Images1," *Academic Radiol.*, vol. 13, no. 1, pp. 63–72, Jan. 2006.

[10] J. Zhou, Y. Zhang, K.-T. Chang, K. E. Lee, O. Wang, J. Li, Y. Lin, Z. Pan, P. Chang, D. Chow, M. Wang, and M.-Y. Su, "Diagnosis of benign and malignant breast lesions on DCE-MRI by using radiomics and deep learning with consideration of peritumor tissue," *J. Magn. Reson. Imag.*, vol. 51, no. 3, pp. 798–809, 2020.

[11] Y. Wang, G. Morrell, M. E. Heibrun, A. Payne, and D. L. Parker, "3D multi-parametric breast MRI segmentation using hierarchical support vector machine with coil sensitivity correction," *Academic Radiol.*, vol. 20, no. 2, pp. 137–147, Feb. 2013.

[12] W.-D. Vogl, K. Pinker, T. H. Helbich, H. Bickel, G. Grabner, W. Bogner, S. Gruber, Z. Bago-Horvath, P. Dubsky, and G. Langs, "Automatic segmentation and classification of breast lesions through identification of informative multiparametric PET/MRI features," *Eur. Radiol. Experim.*, vol. 3, no. 1, pp. 1–13, Dec. 2019.

[13] B. Reig, L. Heacock, K. J. Geras, and L. Moy, "Machine learning in breast MRI," *J. Magn. Reson. Imag.*, vol. 52, no. 4, pp. 998–1018, Oct. 2020.

[14] S. Naz, K. T. Phan, and Y.-P. P. Chen, "A comprehensive review of federated learning for COVID-19 detection," *Int. J. Intell. Syst.*, vol. 37, no. 3, pp. 2371–2392, 2022.

[15] R. Yamashita, M. Nishio, R. K. G. Do, and K. Togashi, "Convolutional neural networks: An overview and application in radiology," *Insights Into Imag.*, vol. 9, no. 4, pp. 611–629, Aug. 2018.

[16] M. U. Dalmış, G. Litjens, K. Holland, and A. Setio, "Using deep learning to segment breast and fibroglandular tissue in MRI volumes," *Med. Phys.*, vol. 44, no. 2, pp. 533–546, 2017.

[17] M. El Adoui, S. A. Mahmoudi, M. A. Larhmam, and M. Benjelloun, "MRI breast tumor segmentation using different encoder and decoder CNN architectures," *Computers*, vol. 8, no. 3, p. 52, Jun. 2019.

[18] X. Ma, J. Wang, X. Zheng, Z. Liu, W. Long, Y. Zhang, J. Wei, and Y. Lu, "Automated fibroglandular tissue segmentation in breast MRI using generative adversarial networks," *Phys. Med. Biol.*, vol. 65, no. 10, May 2020, Art. no. 105006.

[19] C. Li, H. Sun, Z. Liu, and M. Wang, "Learning cross-modal deep representations for multi-modal MR image segmentation," in *Proc. MICCAI*, Shenzhen, China, 2019, pp. 57–65.

[20] J. Zhang, A. Saha, Z. Zhu, and M. A. Mazurowski, "Hierarchical convolutional neural networks for segmentation of breast tumors in MRI with application to radiogenomics," *IEEE Trans. Med. Imag.*, vol. 38, no. 2, pp. 435–447, Feb. 2019.

[21] R. Khaled, J. Vidal, J. C. Vilanova, and R. Martí, "A U-Net Ensemble for breast lesion segmentation in DCE MRI," *Comput. Biol. Med*, vol. 140, Jan. 2022, Art. no. 105093.

[22] W. Yue, H. Zhang, J. Zhou, G. Li, Z. Tang, Z. Sun, J. Cai, N. Tian, S. Gao, J. Dong, Y. Liu, X. Bai, and F. Sheng, "Deep learning-based automatic segmentation for size and volumetric measurement of breast cancer on magnetic resonance imaging," *Frontiers Oncol.*, vol. 12, Aug. 2022, Art. no. 984626.

[23] C. Peng, Y. Zhang, J. Zheng, B. Li, J. Shen, M. Li, L. Liu, B. Qiu, and D. Z. Chen, "IMIIN: An inter-modality information interaction network for 3D multi-modal breast tumor segmentation," *Computerized Med. Imag. Graph.*, vol. 95, Jan. 2022, Art. no. 102021.

[24] G. Piantadosi, S. Marrone, A. Galli, M. Sansone, and C. Sansone, "DCE-MRI breast lesions segmentation with a 3TP U-Net deep convolutional neural network," in *Proc. IEEE 32nd Int. Symp. Comput.-Based Med. Syst. (CBMS)*, Jun. 2019, pp. 628–633.

[25] L. Hirsch, "Radiologist-level performance by using deep learning for segmentation of breast cancers on MRI scans," *Radiol., Artif. Intell.*, vol. 4, no. 1, Jan. 2022, Art. no. e200231.

[26] R. Girshick, J. Donahue, T. Darrell, and J. Malik, "Rich feature hierarchies for accurate object detection and semantic segmentation," in *Proc. IEEE Conf. Comput. Vis. Pattern Recognit.*, 2014, pp. 580–587.

[27] P. Moeskops, J. M. Wolterink, B. HM. Van Der Velden, and K. G. A. Gilhuijs, "Deep learning for multi-task medical image segmentation in multiple modalities," in *Proc. MICCAI*, Athens, Greece, 2016, pp. 478–486.

[28] Y.-Y. Guo, Y.-H. Huang, Y. Wang, J. Huang, Q.-Q. Lai, and Y.-Z. Li, "Breast MRI tumor automatic segmentation and triple-negative breast cancer discrimination algorithm based on deep learning," *Comput. Math. Methods Med.*, vol. 2022, pp. 1–9, Aug. 2022, doi: 10.1155/2022/2541358.

[29] O. Ronneberger, P. Fischer, and T. Brox, "U-Net: Convolutional networks for biomedical image segmentation," in *Proc. MICCAI*, Munich, Germany, 2015, pp. 234–241.

[30] J. Long, E. Shelhamer, and T. Darrell, "Fully convolutional networks for semantic segmentation," in *Proc. IEEE Conf. Comput. Vis. Pattern Recognit.*, Athens, Greece, Jun. 2015, pp. 3431–3440.

[31] Ö. Çiçek, A. Abdulkadir, S. S. Lienkamp, T. Brox, and O. Ronneberger, "3D U-Net: Learning dense volumetric segmentation from sparse annotation," in *Proc. MICCAI*, Athens, Greece, 2016, pp. 424–432.

[32] L. Yu, JZ. Cheng, Q. Dou, and X. Yang, "Automatic 3D cardiovascular MR segmentation with densely-connected volumetric convnets," in *Proc. MICCAI*, Quebec City, QC, Canada, 2017, pp. 287–295.

[33] C. Qin, J. Lin, J. Zeng, Y. Zhai, L. Tian, S. Peng, and F. Li, "Joint dense residual and recurrent attention network for DCE-MRI breast tumor segmentation," *Comput. Intell. Neurosci.*, vol. 2022, pp. 1–16, Apr. 2022.

[34] G. Piantadosi, M. Sansone, R. Fusco, and C. Sansone, "Multi-planar 3D breast segmentation in MRI via deep convolutional neural networks," *Artif. Intell. Med.*, vol. 103, Mar. 2020, Art. no. 101781.

[35] H. Jiao, X. Jiang, Z. Pang, X. Lin, Y. Huang, and L. Li, "Deep convolutional neural networks-based automatic breast segmentation and mass detection in DCE-MRI," *Comput. Math. Methods Med.*, vol. 2020, pp. 1–12, May 2020.

[36] Z. Zhou, M. R. Siddiquee, N. Tajbakhsh, and J. Liang, "UNet++: A nested U-Net architecture for medical image segmentation," in *Proc. Int. Workshop Deep Learn. Med. Image Anal.*, Granada, Spain, 2018, pp. 3–11.

[37] E. D. Carvalho, R. V. Silva, M. J. Mathew, and F. D. Araujo, "Tumor segmentation in breast DCE-MRI slice using deep learning methods," in *Proc. ISCC*, 2021, pp. 1–6.

[38] I. Goodfellow, J. Pouget-Abadie, M. Mirza, B. Xu, and D. Warde-Farley, "Generative adversarial nets," in *Proc. Adv. Neural Inf. Process. Syst.*, vol. 27, 2014, pp. 2–3.
[39] C. Hazirbas, L. Ma, C. Domokos, and D. Cremers, "Fusenet: Incorporating depth into semantic segmentation via fusion-based CNN architecture," in *Proc. Asian Conf. Comput. Vis.*, Taipei, Taiwan, 2017, pp. 213–228.
[40] K. D. Spuhler, J. Ding, C. Liu, J. Sun, M. Serrano-Sosa, M. Moriarty, and C. Huang, "Task-based assessment of a convolutional neural network for segmenting breast lesions for radiomic analysis," *Magn. Reson. Med.*, vol. 82, no. 2, pp. 786–795, Aug. 2019.
[41] M. Ma, L. Gan, Y. Liu, Y. Jiang, L. Xin, Y. Liu, N. Qin, Y. Cheng, Q. Liu, L. Xu, Y. Zhang, X. Wang, X. Zhang, J. Ye, and X. Wang, "Radiomics features based on automatic segmented MRI images: Prognostic biomarkers for triple-negative breast cancer treated with neoadjuvant chemotherapy," *Eur. J. Radiol.*, vol. 146, Jan. 2022, Art. no. 110095.
[42] L. Gan, M. Ma, Y. Liu, and Q. Liu, "A clinical–radiomics model for predicting axillary pathologic complete response in breast cancer with axillary lymph node metastases," *Frontiers Oncol.*, vol. 11, Dec. 2021, Art. no. 786346.
[43] J. Ying, R. Cattell, T. Zhao, L. Lei, Z. Jiang, S. M. Hussain, Y. Gao, H.-H.-S. Chow, A. T. Stopeck, P. A. Thompson, and C. Huang, "Two fully automated data-driven 3D whole-breast segmentation strategies in MRI for MR-based breast density using image registration and U-Net with a focus on reproducibility," *Vis. Comput. Ind., Biomed., Art*, vol. 5, no. 1, p. 25, Oct. 2022.
[44] Y. Nam, G. E. Park, J. Kang, and S. H. Kim, "Fully automatic assessment of background parenchymal enhancement on breast MRI using machine-learning models," *J. Magn. Reson. Imag.*, vol. 53, no. 3, pp. 818–826, Mar. 2021.
[45] Y. Zhang, S. Chan, V. Y. Park, K.-T. Chang, S. Mehta, M. J. Kim, F. J. Combs, P. Chang, D. Chow, R. Parajuli, R. S. Mehta, C.-Y. Lin, S.-H. Chien, J.-H. Chen, and M.-Y. Su, "Automatic detection and segmentation of breast cancer on MRI using mask R-CNN trained on non–fat-sat images and tested on fat-sat images," *Academic Radiol.*, vol. 29, pp. S135–S144, Jan. 2022.
[46] A. Galli, S. Marrone, G. Piantadosi, M. Sansone, and C. Sansone, "A pipelined tracer-aware approach for lesion segmentation in breast DCE-MRI," *J. Imag.*, vol. 7, no. 12, p. 276, Dec. 2021.
[47] A. Gubern-Mérida, M. Kallenberg, R. M. Mann, R. Martí, and N. Karssemeijer, "Breast segmentation and density estimation in breast MRI: A fully automatic framework," *IEEE J. Biomed. Health Informat.*, vol. 19, no. 1, pp. 349–357, Jan. 2015.
[48] K. Dutta, S. Roy, T. D. Whitehead, J. Luo, A. K. Jha, S. Li, J. D. Quirk, and K. I. Shoghi, "Deep learning segmentation of triple-negative breast cancer (TNBC) patient derived tumor xenograft (PDX) and sensitivity of radiomic pipeline to tumor probability boundary," *Cancers*, vol. 13, no. 15, p. 3795, Jul. 2021.
[49] V. Badrinarayanan, A. Kendall, and R. Cipolla, "SegNet: A deep convolutional encoder–decoder architecture for image segmentation," *IEEE Trans. Pattern Anal. Mach. Intell.*, vol. 39, no. 12, pp. 2481–2495, Dec. 2017.
[50] P. Oza, P. Sharma, S. Patel, and P. Kumar, "Deep convolutional neural networks for computer-aided breast cancer diagnostic: A survey," *Neural Comput. Appl.*, vol. 34, no. 3, pp. 1815–1836, Feb. 2022.
[51] K. Kamnitsas, C. Ledig, V. F. J. Newcombe, J. P. Simpson, A. D. Kane, D. K. Menon, D. Rueckert, and B. Glocker, "Efficient multi-scale 3D CNN with fully connected CRF for accurate brain lesion segmentation," *Med. Image Anal.*, vol. 36, pp. 61–78, Feb. 2017.
[52] K. Simonyan and A. Zisserman, "Very deep convolutional networks for large-scale image recognition," 2014, *arXiv:1409.1556*.
[53] S. Wang, X. Hou, and X. Zhao, "Automatic building extraction from high-resolution aerial imagery via fully convolutional encoder–decoder network with non-local block," *IEEE Access*, vol. 8, pp. 7313–7322, 2020.
[54] N. Srivastava, G. Hinton, A. Krizhevsky, I. Sutskever, and R. Salakhutdinov, "Dropout: A simple way to prevent neural networks from overfitting," *J. Mach. Learn. Res.*, vol. 15, no. 1, pp. 1929–1958, 2014.
[55] G. Maicas, G. Carneiro, and A. P. Bradley, "Globally optimal breast mass segmentation from DCE-MRI using deep semantic segmentation as shape prior," in *Proc. IEEE 14th Int. Symp. Biomed. Imag. (ISBI)*, Apr. 2017, pp. 305–309.
[56] X. Meng, J. Fan, H. Yu, J. Mu, Z. Li, A. Yang, B. Liu, K. Lv, D. Ai, Y. Lin, H. Song, T. Fu, D. Xiao, G. Ma, J. Yang, and Y. Gu, "Volume-awareness and outlier-suppression co-training for weakly-supervised MRI breast mass segmentation with partial annotations," *Knowl.-Based Syst.*, vol. 258, Dec. 2022, Art. no. 109988.
[57] K. Wang, A. Mamidipalli, T. Retson, N. Bahrami, K. Hasenstab, K. Blansit, E. Bass, T. Delgado, G. Cunha, M. S. Middleton, R. Loomba, B. A. Neuschwander-Tetri, C. B. Sirlin, and A. Hsiao, "Automated CT and MRI liver segmentation and biometry using a generalized convolutional neural network," *Radiol., Artif. Intell.*, vol. 1, no. 2, Mar. 2019, Art. no. 180022.
[58] M. Ghafoorian, A. Mehrtash, T. Kapur, and N. Karssemeijer, "Transfer learning for domain adaptation in MRI: Application in brain lesion segmentation," in *Proc. MICCAI*, Quebec City, QC, Canada, 2017, pp. 516–524.
[59] L. Abdelrahman, M. Al Ghamdi, F. Collado-Mesa, and M. Abdel-Mottaleb, "Convolutional neural networks for breast cancer detection in mammography: A survey," *Comput. Biol. Med.*, vol. 131, Apr. 2021, Art. no. 104248.

KHADIJEH ASKARIPOUR received the M.S. and Ph.D. degrees in structural engineering from the Shahid Bahonar University of Kerman, Iran, in 2012 and 2019, respectively. From 2017 to 2018, she was a Visiting Researcher with the Faculty of Electrical and Control Engineering, Gdańsk University of Technology, Gdańsk, Poland. Since 2021, she has been an Assistant Professor with the Department of Biomechatronics, Gdańsk University of Technology. Her research interests include machine learning, health monitoring, data processing, and structural dynamics.

ARKADIUSZ ZAK received the M.Sc. degree from the Faculty of Technical Physics and Applied Mathematics of the Gdansk University of Technology in 1989, the Ph.D. degree in the field of machine dynamics in 1998, and the D.Sc. degree from the Polish Academy of Sciences, Gdansk, U.K., in 2009. As a final-year student, he began his research at the Polish Academy of Sciences, Gdansk. From 2000 to 2003, he worked as a postdoc at the Dynamics Laboratory at the University of Glasgow. From 2003 to 2012, he worked at the Polish Academy of Sciences in Gdansk. In 2012, he joined the research group at the Department of Biomechatronics, Gdansk University of Technology, where he currently works. His research interests are broad, focusing mainly on modelling physical phenomena using the finite element method, as well as on issues related to structural health monitoring. His work also concerns damage modelling, smart and metamaterials, periodic structures, and more recently various aspects of bioengineering.